Supporting Information

Rotational Dynamics of Li^+ Ions Encapsulated in C_{60} Cages at Low Temperatures

Hal Suzuki,* Misaki Ishida, Masatsugu Yamashita, Chiko Otani, Kazuhiko Kawachi, Yasuhiko Kasama, Eunsang Kwon

Sample preparation

$[Li^+@C_{60}](PF_6^-)$ was synthesized at Idea International Co. Ltd., Japan, using a plasma method.[1] The sample purity was assessed using elemental analysis and F^{19}-NMR. The carbon content of C_{60} and the presence of hydrogen and nitrogen impurities were determined by elemental analysis using an MT-6 CHN analyzer (YANACO). Theoretical content: C, 82.59%; N, 0%; H, 0%. Found: C, 82.57%, N, 0.31%, H, 0.28%. The phosphorus content of the PF_6^- ions was determined using F^{19}-NMR. Theoretical content: 3.55%. Found: 3.12%. These results confirmed that the sample purity was >88%.

The crystal structure and crystallinity of the sample were verified by powder X-ray diffraction (XRD) measurements using a D2 PHASER (Bruker) (Fig. S1(a)). The XRD pattern showed sharp peaks at the same positions to those calculated from the single crystal data determined by Aoyagi et al.[2] A low crystallinity sample, which showed diffuse XRD peaks, was also obtained accidentally by recrystallization from *o*-dichlorobenzene solution using *n*-hexane as a poor solvent (Fig. S1(a)).

THz spectroscopy

Terahertz (THz) absorption spectra were obtained using three different spectrometers. The spectrum at 300 K was obtained by Fourier-transform far-infrared (FT-FIR) spectrometer (FARIS JASCO) equipped with a high-pressure mercury lamp, wire-grid beam splitter, and superconducting bolometer (QMC Instruments). The spectra at low temperatures (10–300 K) were obtained using a terahertz time-domain spectrometer (THz-TDS) and an FT-FIR spectrometer (DA8 PC.2SCV, Bomen). The THz-TDS was used for measurement between 0.5 and 1.8 THz, while the FT-FIR spectrometer was used for measurement between 1.8 and 4.0 THz. The THz-TDS system was constructed by ourselves: A conventional transmission geometry was adopted, and photoconductive antennae and a Ti:sapphire laser (Coherent Vitesse: pulse width ~100 fs, repeat rate 80 MHz, average power ~1 W) were utilized to generate and detect THz pulses. The temperature was controlled using a helium flow cryostat (OptistatCF2, Oxford Instruments) equipped with a

polyethylene window. The sample temperature was calibrated using a Au/Fe-chromel thermocouple.

The crystalline sample was pressed to form a pellet ~4 mm in diameter and ~0.1 mm in thickness. For the FT-FIR measurements at low temperatures, the sample was diluted in pure C_{60} crystals (2.23 wt%), since the absorbance peak at ~2.3 THz was too intense to be measured without dilution. Pure C_{60} did not show any peaks in this frequency range (Fig. S1(b)).

Assignment of spectral peaks

In the THz frequency range, two types of motions were expected to be observed for $[Li^+@C_{60}](PF_6^-)$ crystal: the lattice vibration of a rock-salt-type crystal and the vibration or rotation of the C_{60}-encaged Li^+ ions. The spectral peaks observed experimentally were assigned utilizing the results obtained from the low-crystallinity sample. The peak at ~2.3 THz showed significant dependence on the crystallinity, which indicated that it was the band corresponding to the lattice modes (Fig. S1(b)). Conversely, the peak at ~1.2 THz was independent of the crystallinity, showing that this is an isolated mode, i.e., the motion of Li^+ ions in the C_{60} cages. Given the fact that the Li^+ ion is distributed on a spherical shell with radius ~1.5 Å,[2] the three modes for the Li^+ ion can be classified into a radial mode and two rotational modes. Previous theoretical works predicted that the radial vibration would have a resonance frequency at ~12 THz and rotational (librational) modes lower than 5 THz.[3] In addition, the free-rotation model predicted that bands would appear at ~0.6 THz. Considering all these, we concluded that the peak at ~1.2 THz corresponded to the rotational motion of the Li^+ ion.

Temperature dependence of THz spectra

The broad peak at ~1.2 THz shifts to lower frequency with decreasing temperature, which was semi-quantitatively explained using the free-rotation model (a detailed description of the free-rotation model is given in the main text). The temperature variation of the peak top frequency is given in Fig. S2 (filled circles). The frequency of the most intense band among the theoretical free rotation bands is also given in Fig. S2 (open circles). These frequency changes present similar slopes above 100 K. The slopes differ below 100 K, where the Li^+ ion starts localizing into two positions.

The sharp peak at ~2.3 THz shifts to higher frequency with decreasing temperature, which was explained in relation to the anharmonicity of the lattice vibration.[4] The temperature variation in the peak frequency (filled circles) and lattice constant[2] (open circles) is given in Fig. S3. The lattice shrinks with decreasing temperature and the vibrational band shifts to higher frequency above 100 K. However, the band does not shift at low temperatures (<100 K), indicating that the vibration becomes harmonic.

The spectral peaks change in intensity with temperature. The broad peak at ~1.2 THz disappears at low temperatures, while new peaks appear at 2.2 and 2.65 THz (Fig. 2(d)). Since separation of the peaks was not successful, the peak intensities were evaluated by calculating the spectral area between 0.5 and 1.8 THz for the peak at 1.2 THz (Fig. 4(a)), and between 1.8 and 3.0 THz for the peak at 2.3 THz (Fig. 4(b)). The former decreases with decreasing temperature, while the latter increases.

These intensity variations were explained by a simple Li^+ rotation energy scheme (Fig. 3(b)). The scheme was obtained by modifying the free-rotation model, i.e., the lowest two rotational levels (l = 0 (singlet) and l = 1 (triplet)) were changed to a librational level. The librational level is fourfold degenerate since the Li^+ ion localizes into two positions, and at each position the librational level is doubly degenerate corresponding to the modes along θ and ϕ direction. The energy gap between the librational level and the lowest rotational level (l = 2) was set to 2.2 THz. The THz spectra calculated from this scheme reproduced the experimental results well, i.e., the rotational bands shift to lower frequency with decreasing temperature and disappear below 100 K, while a sharp peak emerges at 2.2 THz (Fig. S4). The spectral intensities were also reproduced by this model, i.e., the occupancies of rotational or librational states were shown to be proportional to the peak intensities observed (Fig. 4).

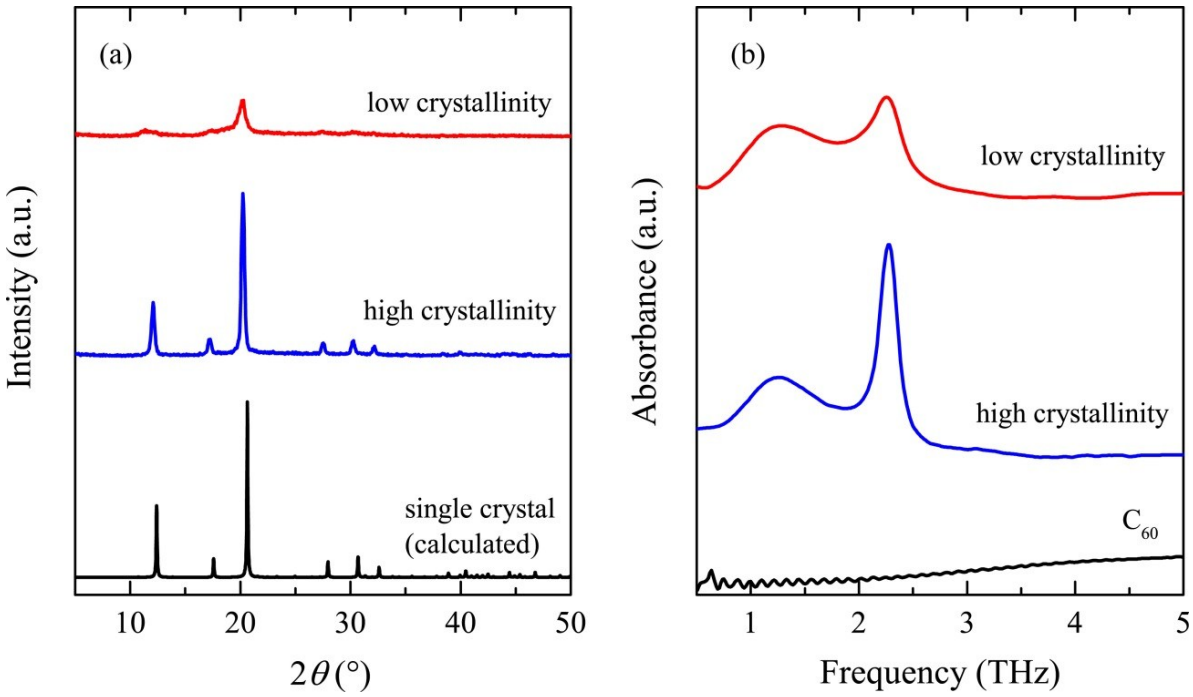

Fig. S1 (a) Powder XRD pattern of $[Li^+@C_{60}](PF_6^-)$ crystals. The high-crystallinity sample measured in this study shows sharp Bragg peaks (blue) at the same positions to those calculated from the single-crystal data obtained by the preceding study (black).[2] The sample with low crystallinity shows diffuse peaks (red). (b) THz spectrum of $[Li^+@C_{60}](PF_6^-)$ crystals. The high-crystallinity sample measured in this study shows a sharp peak at 2.3 THz, while the low-crystallinity sample shows a broad peak. Pure C_{60} crystals do not show any peaks in this frequency range (black).

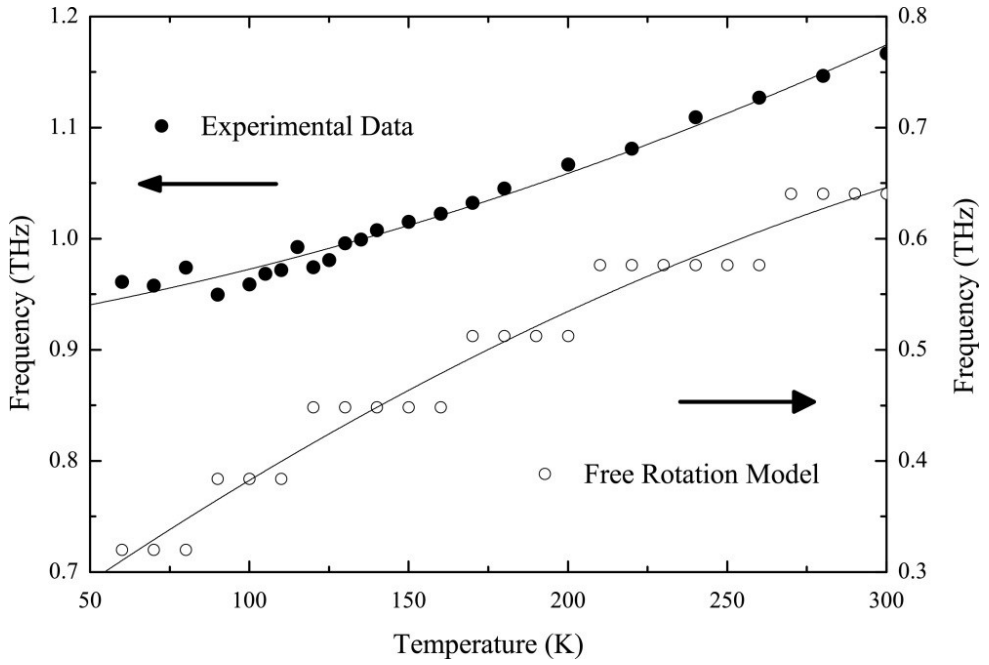

Fig. S2 Temperature dependence of the frequency of the broad spectral peak at ~1.2 THz (filled circles), and that of the most intense band of the free-rotation model (open circles). The curves are the guide to eye.

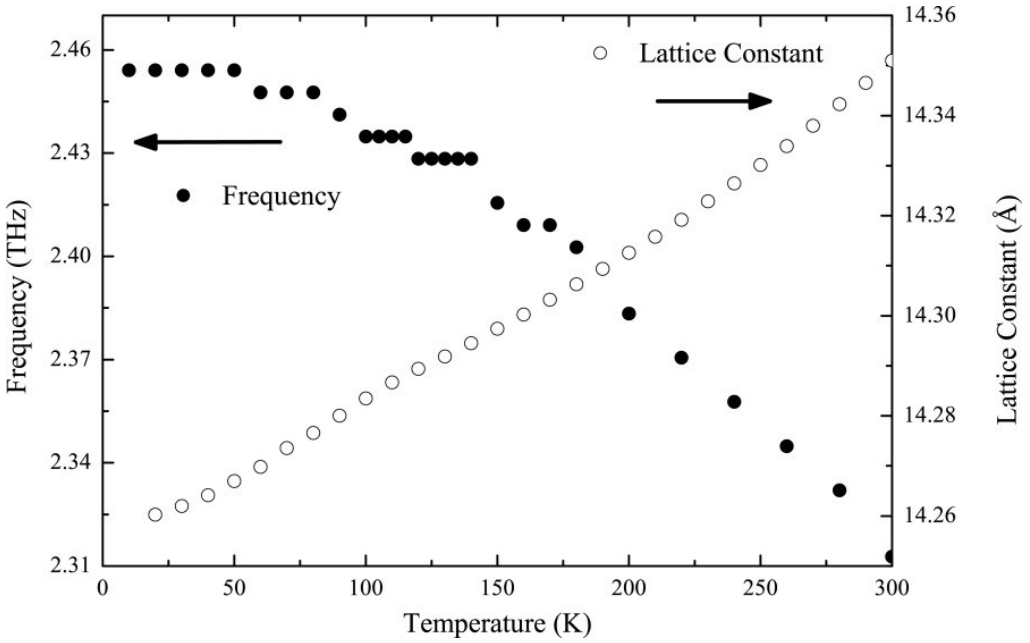

Figure S3. Temperature dependence of the frequency of the sharp peak at ~2.3 THz (filled circles). Temperature-dependent lattice constants (open circles) are also given as a reference.[2]

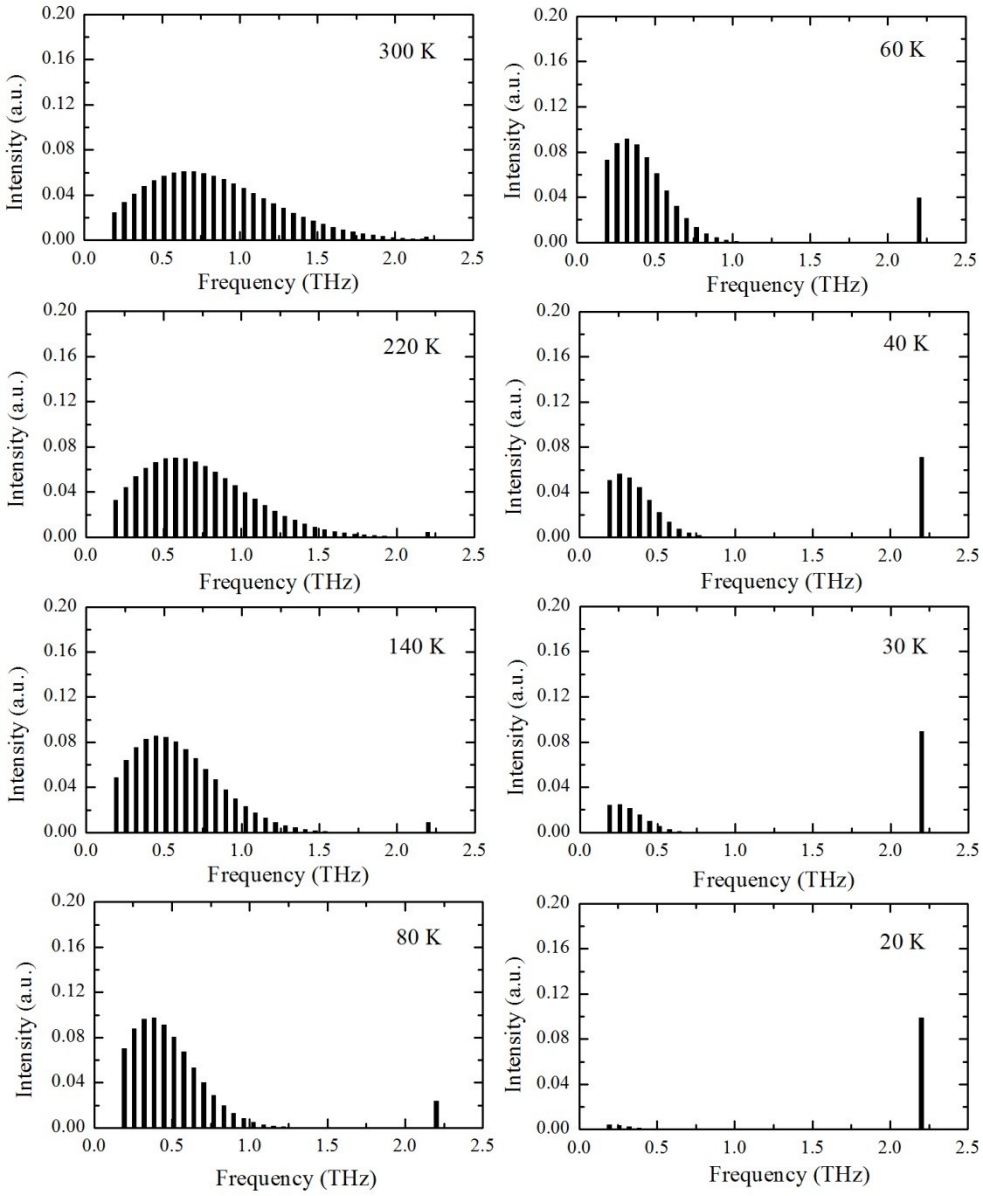

Fig. S4 THz spectra calculated from the energy scheme in Fig. 3(b) at several temperature points. The rotational bands (0–2.0 THz) decrease in intensity with decreasing temperature while a librational band emerges at 2.2 THz. The relative intensities of the rotational and librational bands are arbitrarily scaled.

References

[1] H. Okada, T. Komuro, T. Sakai, Y. Matsuo, Y. Ono, K. Omote, K. Yokoo, K. Kawachi, Y. Kasama, S. Ono, R. Hatakeyama, T. Kaneko, H. Tobita, *RSC Adv.*, 2012, **2**, 10624.

[2] S. Aoyagi, Y. Sado, E. Nishibori, H. Sawa, H. Okada, H. Tobita, Y. Kasama, R. Kitaura, H. Shinohara, *Angew. Chem. Int. Ed.*, 2012, **51**, 3377.

[3] M. Zhang, L. B. Harding, S. K. Gray, S. A. Rice, *J. Chem. Phys. A*, 2008, **112**, 5478.

[4] M. A. White, C. Meingast, W. I. F. David, T. Matsuo, *Solid State Commun.*, 1995, **94**, 481.